Project 1

Simulation of Rayleigh Fading

CES 544 – Wireless Communication
Sonoma State University
Spring 2007

David Bozarth

Introduction

Signal impairments in the wireless channel arise both from propagation effects, which are unique to wireless communication; and from noise and interference, which are common to many electromagnetic communication systems. In mobile wireless communications, the term "fading" denotes variation of received signal amplitude and phase, with respect to both time and distance. Small-scale fading results from interaction between the propagating wavefront, the mobile receiver, and nearby objects. Modeling of this dynamic interaction system must consider Doppler frequency effects.

Consideration of multipath time delay may also be required. If the maximum spread of time delay (τ_{max}) between multipath signal components is much less than the symbol period T_s, then relative multipath delay can be ignored - all multipath components may be regarded as one with respect to time. This condition is called "flat" or non-frequency-selective fading, because the channel coherence bandwidth (over which the channel is strongly autocorrelated) is wide (the curve is flat) compared with the signal bandwidth.

In a hilly or dense urban environment, no line-of-sight signal component is likely to reach the receiver. Scattering of the wavefront by many nearby objects is expected. Consequently the received signal is regarded as equally probable from any direction. This condition is termed isotropic scattering, and may be modeled using a Rayleigh distribution, wherein the random variable

$$Z = \mathrm{sqrt}(X^2 + Y^2)$$

is a function of two independent, zero-mean, normally distributed random variables X and Y. Small-scale fading in such a system is termed Rayleigh fading. In a flat Rayleigh fading model, X and Y represent the in-phase and quadrature components of the channel impulse response. These are both random processes – so that the resultant envelope Z is also a random process.

The Jakes sum-of-sinusoid method was used with Matlab to simulate flat Rayleigh fading, and statistical properties of the simulated fading channel were investigated. Appendix 1 (*Project 1 Procedure*) gives details of the theory and procedure.

Core implementation

Equations 1 – 3 in Appendix 1 were implemented as an mfile:

```
function [X] = Rayleigh_sub(N, f, T, M)
% Returns a simulated Rayleigh distribution [2, N] representing the time
% variable with complex value of a distribution with N samples.
% f is the max Doppler frequency.
% T is the time period of sampling.
% M is a constant, usually 8 or 16.
%
% 03-12-07 D.Bozarth, Engineering Science Dept, Sonoma State University.

% Initialize the return value array.
X = zeros(2, N); % Col 1: time value, Col 2: complex value

% Generate a uniform RV representing a constant angle for each sample.
theta = rand(1, 1) * 2 * pi;

    % Generate uniform RV's representing constant angles for each summation point.
    alpha = rand(1, M) * 2 * pi;
    beta  = rand(1, M) * 2 * pi;

% Obtain each time value, and each corresponding complex value.
for n = 1:N % Each sample

    % Calculate the time value corresponding to this sample.
    Tn = T * (n - 1);
    X(1, n) = Tn;

    % Calculate a single sample complex value.
    m = 1:M;
    z = 2 * pi * f * cos(( (2 * m - 1) * pi + theta ) / (4 * M) ) * Tn;
    Y(m) = cos(z + alpha(m)) + i * sin(z + beta(m));
    X(2, n) = sum(Y) / sqrt(M);
end

% end of program
```

For each of the reported simulations, the size of M was specified as 16, and the value of T was fixed at 100 μs.

Results

For both the in-phase and quadrature components $h_I(t)$ and $h_Q(t)$, the expected value of the square of each component is 0.5. The variance is given as the expected value of the real component, or 0.5.

With N = 400 and f_D = 100 Hz, the simulator returned channel response characterized in the following plots.

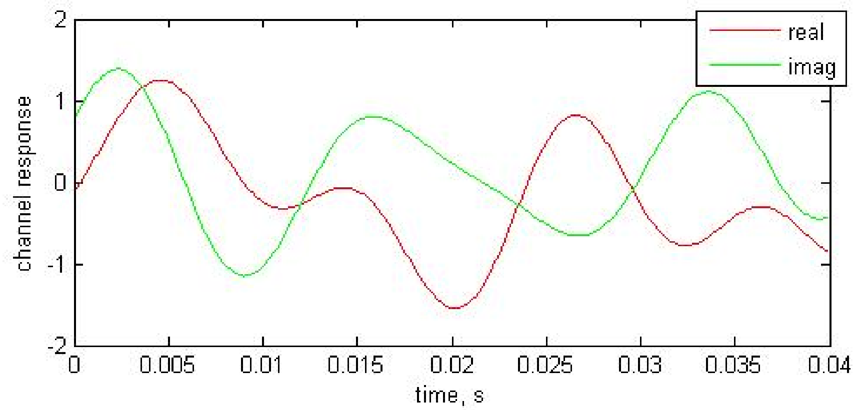

Fig. 1: Complex impulse response of the channel (N = 400, f_d = 100 Hz)

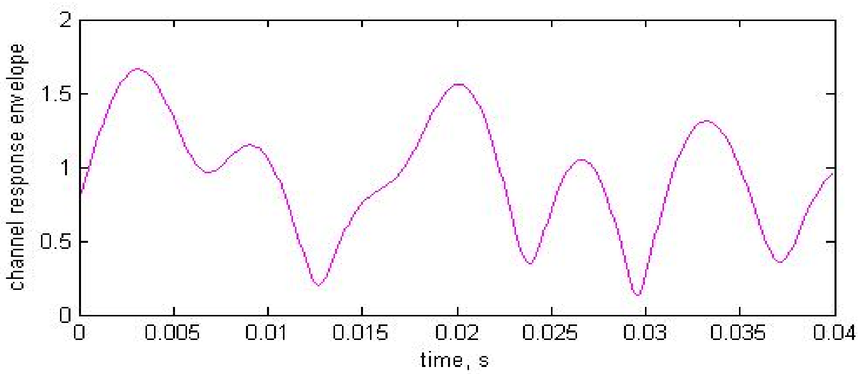

Fig. 2: Envelope of impulse response (N = 400, f_d = 100 Hz)

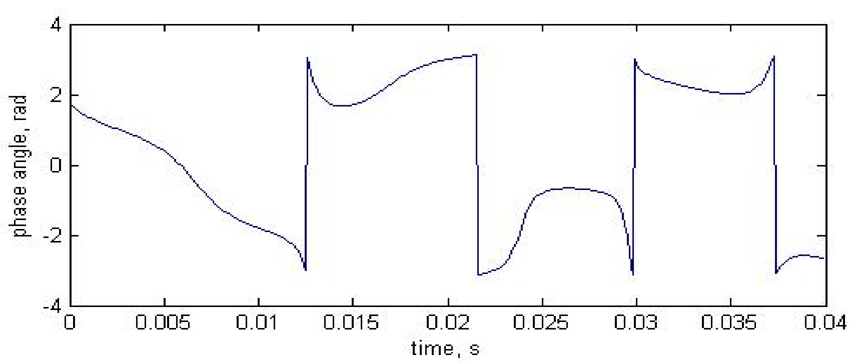

Fig. 3: Angle of impulse response (N = 400, f_d = 100 Hz)

With N = 400 and f_D = 10 Hz, the simulator returned a less rapidly-changing channel response over the same sampling range. This exhibits improved time-domain correlation of the impulse response relative to the previou case (f_D = 100 Hz).

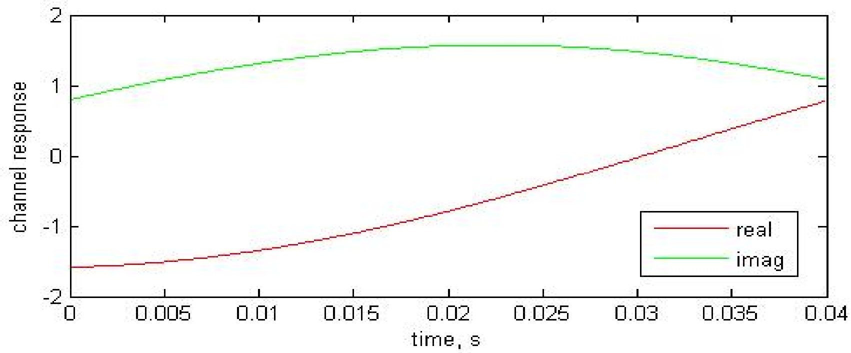

Fig. 4: Complex impulse response of the channel (N = 400, f_d = 10 Hz)

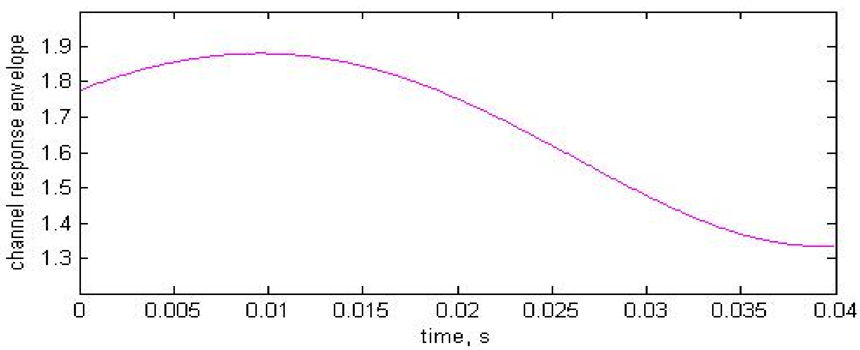

Fig. 5: Envelope of impulse response (N = 400, f_d = 10 Hz)

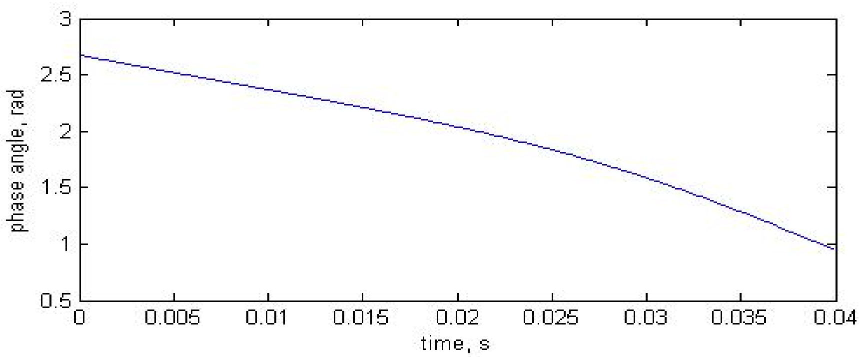

Fig. 6: Angle of impulse response (N = 400, f_d = 10 Hz)

Accordingly, after increasing f_D to 300 Hz we see a more rapidly changing channel (very small autocorrelation magnitude). Formally, the autocorrelation is specified by half the product of channel power with a zero-order Bessel function of the first kind,

$$R_{ZZ} = P\, J_0(2\pi f_D T_n) / 2$$

where $J_0(x)$ evaluates as an alternating series of terms with increasing powers of x in each numerator. The limit of the Bessel function of the first kind is zero with infinite x; both its alternation frequency and damping factor are determined by f_D. Thus the autocorrelation magnitude gets "smaller, faster" with increasing f_D. This means a more rapidly-changing impulse response seen in the real and imaginary components, in the envelope, and in the phase angle.

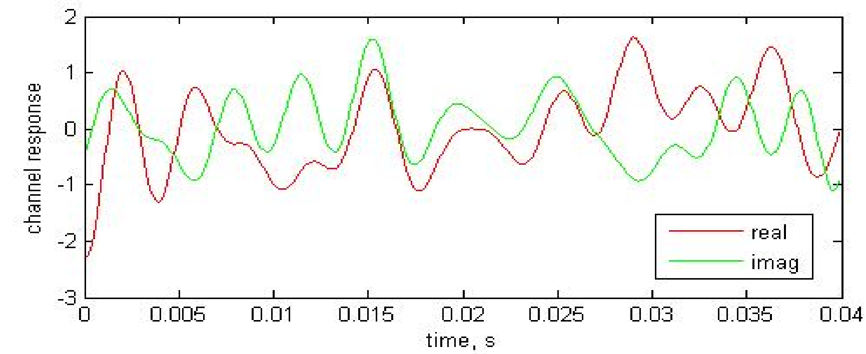

Fig. 7: Complex impulse response of the channel (N = 400, f_d = 300 Hz)

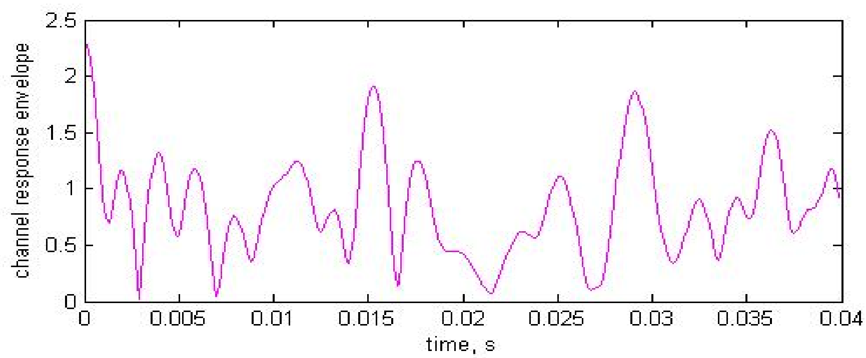

Fig. 8: Envelope of impulse response (N = 400, f_d = 300 Hz)

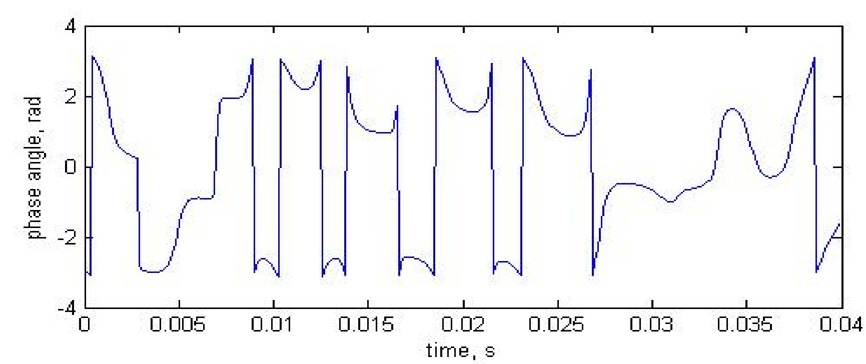

Fig. 9: Angle of impulse response (N = 400, f_d = 300 Hz)

Statistical properties

Using N = 100,000 and f_D = 100 Hz, the sample means of the real and imaginary components were each on the order of 10^{-3} – very close to the theoretical value of 0. Similarly, the measured variance of each component was within about 10^{-3} of the theoretical value of 0.5.

The real and imaginary component pdf's were each compared with the theoretical density:

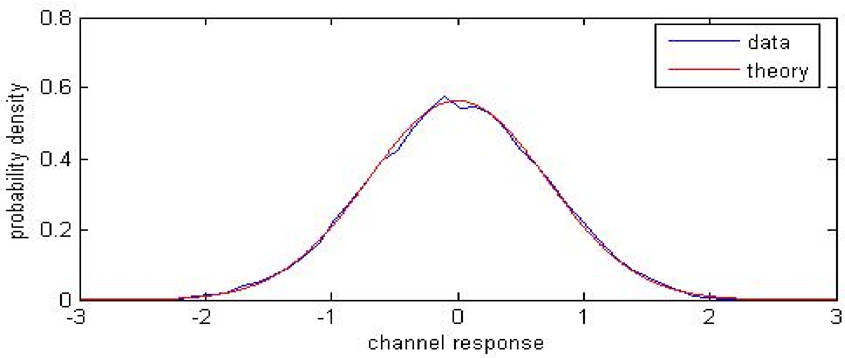

Fig 10: Density of real component (N = 100,000, f_D = 100 Hz)

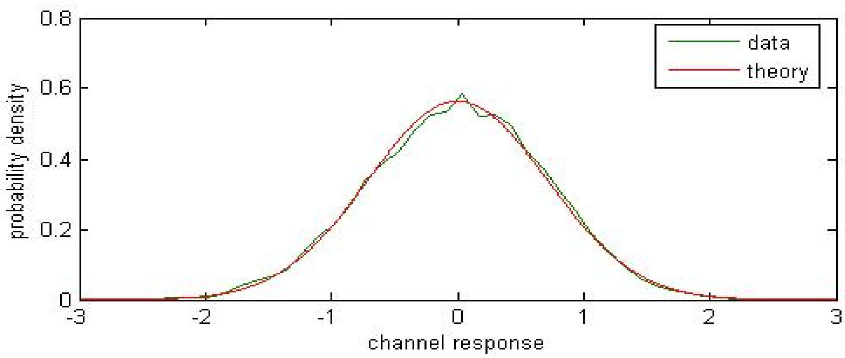

Fig 11: Density of imaginary component (N = 100,000, f_D = 100 Hz)

The envelope pdf was compared with the theoretical Rayleigh distribution using variance 0.5:

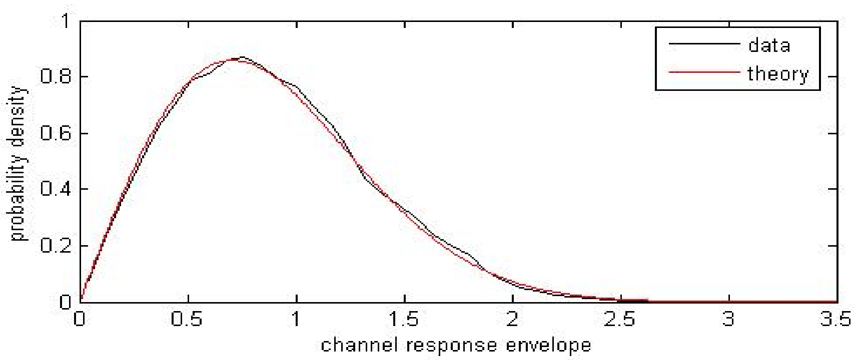

Fig 12: Density of Rayleigh flat fading envelope (N = 100,000, f_D = 100 Hz)

Using N = 1000 and f_D = 180 Hz, the correlation matrix and its ensemble average were found according to Appendix 1. The resulting autocorrelation function had a maximum value of 1000. The non-negative portion of the real component of this function was normalized to a maximum value of 1, and plotted on the same graph with the real component of theoretical autocorrelation obtained with a Bessel function. The Matlab steps not given in Appendix 1, and the resulting graph are shown:

```
mu = zeros(2, 1999);
t = -999:999;
mu(1, :) = t .* T;
mu(2, :) = mean(real(corr_mat), 1);
plot(mu(1, 1000:1999), mu(2, 1000:1999) ./ 1000);
bh = besselj(0, 2 * pi * f * h(1, :));
hold on;
plot(h(1, :), bh, '-r');
```

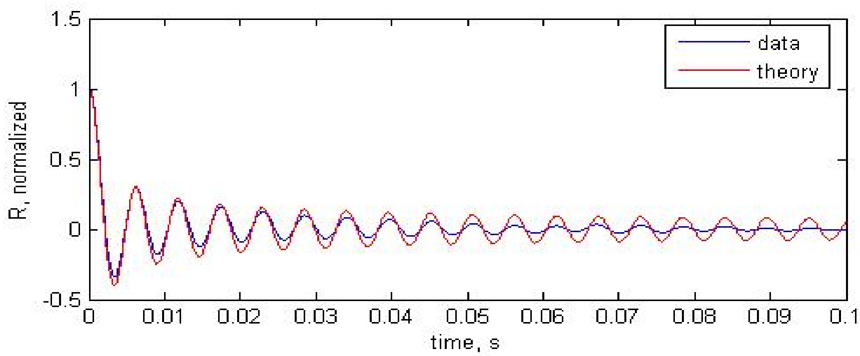

Fig 13: Real component of autocorrelation of Rayleigh flat fading envelope (N = 1000, f_D = 180 Hz)

Excess damping of the data obtained from the simulation is in evidence. The discussion on p.85 of our text, and the graph on p.86, indicate that such deviation for large time lags is to be expected from the Jakes sum-of-sinusoid simulation method. This phenomenon is associated with a finite number (M) of oscillators used in the simulation, and represents the analog of excess mass in a physical harmonic oscillator, or excess resistance in an electrical oscillator.

Conclusion

A Rayleigh flat-fading channel was simulated using the sum-of-sinusoids method. Maximum Doppler frequency was varied, and the effect of this variation on received signal properties was demonstrated. Non-ideal behavior of the simulation was shown with regard to time-domain correlation over relatively large time periods.